RSC Advances

ROYAL SOCIETY OF CHEMISTRY

www.rsc.org/advances

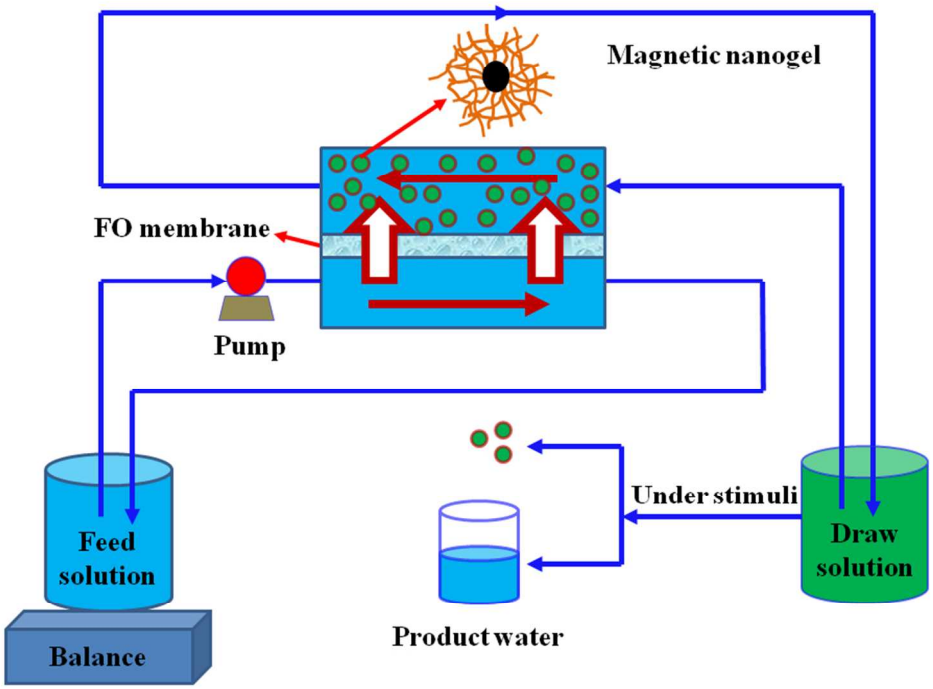

254x190mm (96 x 96 DPI)

Cite this: DOI: 10.1039/c0xx00000x

www.rsc.org/xxxxxx

ARTICLE TYPE

Magnetic Thermoresponsive Ionic Nanogels as Novel Draw Agents in Forward Osmosis

Aijiao Zhou[a], Huayong Luo[a], Qin Wang*[b], Lin Chen[a], Tian C. Zhang[c], and Tao Tao[a]

Received (in XXX, XXX) Xth XXXXXXXXX 20XX, Accepted Xth XXXXXXXXX 20XX

DOI: 10.1039/b000000x

Magnetic poly(*N*-isopropylacrylamide-*co*-sodium 2-acrylamido-2-methylpropane sulfonate) (denoted as Fe_3O_4@P(NIPAM-*co*-AMPS)) nanogels were prepared based on strong ionic monomer AMPS and thermosensitive monomer NIPAM *via* precipitation polymerization at the present of Fe_3O_4 nanoparticles and investigated as draw solutes in FO. The magnetic nanogels were characterized by Fourier-transform infrared spectrum, transmission electron microscopy, dynamic light scattering, X-ray diffraction, and vibrating sample magnetometer, respectively, indicating that they exhibited a core-shell structure, thermosensitivity and superparamagnetic property. These properties would benefit to recover these nanogels after FO. The water flux yielded by Fe_3O_4@P(NIPAM-*co*-AMPS) nanogels in FO was investigated compared with magnetic weak ionic nanogels based on poly(*N*-isopropylacrylamide-*co*-acrylic acid) under the same operating conditions. The results show that the water flux yielded by Fe_3O_4@P(NIPAM-*co*-AMPS) nanogels is 2.4 times higher than the later. Furthermore, the water flux increases with the increase of nanogels concentration in the draw solution. Especially, due to the existence of thermosensitive poly(*N*-isopropylacrylamide) segments in Fe_3O_4@P(NIPAM-*co*-AMPS) nanogels, these nanogels can be recovered from the diluted draw solution quickly under an external magnetic field combined with a thermal stimuli, resulting in an improvement of the recovery efficiency.

Introduction

Forward osmosis (FO) is a kind of membrane separation process driven by the inherit osmotic pressure of a draw solution, which is higher than that of a feed solution. Although FO has been regarded as a promising and sustainable non-traditional membrane technology,[1-3] one of the main obstacles for the sustainable development of FO technology is the absence of suitable draw agents with high osmotic pressure, low reverse solute flux, and easy recovery.[4,5] At present, ammonia/carbon dioxide (CO_2/NH_3) solution has been regarded as the most promising draw agent in FO proposed by Elimelech *et al*. with high osmotic pressure and low-energy consumption for recovery as low as an electrical power of less than 0.25 kWh/m^3.[6,7] However, CO_2/NH_3 solution may cause significant reverse solute diffusion, and the removal of ammonia residue from product water still remains a critical issue. So far, a lot of small molecule compounds have been proposed as draw solutes, including aluminum sulfate,[8] fertilizers,[9] organic ionic salts (*e.g.*, magnesium acetate and sodium propionate),[10] 2-methylimidazole-based compounds,[11] switchable polarity solvents,[12] hexavalent phosphazene salts,[13] hydroacid complexes,[14] sodium lignin sulfonate,[15] EDTA sodium salts,[16] and zwitterions[17] besides traditional draw solutes like sodium chloride. Although these draw solutes can produce high osmotic pressure due to their low molecular weight or highly-charged groups, they tend to induce high reverse solute flux or are usually separated from product water or re-concentrated for reuse at an intensive energy cost.

To reduce the energy consumption for draw solute recovery after FO, some novel draw solutes with intelligent responding properties have attracted growing concerns, including functionalized magnetic nanoparticles (MNPs),[18-24] thermo-responsive polyelectrolytes,[25] and stimuli-responsive hydrogels responding to different stimuli like temperature,[26,27] a combination of temperature and hydraulic pressure,[28] sunlight,[29-32] gas pressure,[33] and magnetic heating[34]. These intelligent draw solutes could be recovered at a relative low-energy cost under an external stimulus such as magnetic field, heating, sunlight or pressure.[35] Meanwhile, a minimal reverse solute flux of draw solute could be obtained due to their big sizes. To achieve a high water flux, they were usually incorporated with ionic groups in their chemical structures. For example, Li *et al.*[28] investigated poly(*N*-isopropylacrylamide-*co*-sodium acrylate) [P(NIPAM-*co*-SA)] hydrogels composed of ionic monomer SA and temperature-sensitive monomer NIPAM as draw solutes in FO. Our group also investigated the copolymerized hydrogels based on strong ionic monomer sodium 2-acrylamido-2-methylpropane sulfonate (AMPS) and thermosensitive monomer NIPAM as draw agents.[27] As we know, poly(*N*-isopropylacrylamide)-based hydrogels are the most investigated thermosensitive hydrogels, which are swollen in water below their volume phase transition temperature (VPTT) and expel water from their network above their VPTT.[36] These intelligent hydrogels can be dewatered quickly by a

combined stimulus of heating and hydraulic pressure.[28] However, they were usually used in the form of bulk gel with large particle sizes (50-150 μm),[28] leading to the slow hydrogels' movement or water transferring within these hydrogels in FO. As well, the hydrogels contacted with the membrane are diluted immediately by water and hence the driving force is lowered, resulting in the external concentration polarization (ECP), which should be avoided during FO. Recently, Chung's group[19,21] and Bai *et al.*[18] explored highly hydrophilic Fe_3O_4 nanoparticles (d = 20-30 nm) coated with water-absorbing linear polymers such as poly(acrylic acid) (PAA), poly(ethylene glycol) diacid (PEG-$(COOH)_2$), PNIPAM and dextran as draw solutes in FO, which would inhibit ECP happened due to their movelity and be recovered under a magnetic field. However, the coatings on these MNPs are all linear polymers with neutral or weak polarity, resulting in a limited osmotic pressure and water-absorbing capacity. Furthermore, the linear polymer layers coated on Fe_3O_4 nanoparticles are too thin to inhibit MNPs' aggregation, which limit their reuse.

As reported, nanogels are formed with a three-dimensional network of polymer chains, and the particle size ranges from several to hundreds of nanometers.[37] They are able to absorb a large amount of water, and response to kinds of stimuli through their chemical structure design, which have been studied extensively in drug controlled release,[38] catalysis[39] and so on. In addition, compared with linear polymers, the dispersion of nanogels has a relative lower viscosity, even at a high concentration.[40] These characteristics of nanogels may be beneficial for use in the FO system.

This work is to develop magnetic thermoresponsive ionic nanogels based on poly(*N*-isopropylacrylamide-*co*-sodium 2-acrylamido-2-methylpropane sulfonate) [P(NIPAM-*co*-AMPS)] and to evaluate these nanogels as draw agents in FO. As the MNPs are coated with a dense layer formed by gel network, it is expected to prevent the aggregation of magnetic nanogels. Besides, these nanogels may generate higher osmotic pressure due to the strong ionic monomer AMPS copolymerized with NIPAM on the surface of MNPs. Furthermore, the presence of thermosensitive PNIPAM in the nanogels may promise a faster separation of nanogels from product water under both thermal and magnetic field stimuli.

Experimental

Materials

Ferric chloride hexahydrate ($FeCl_3$•$6H_2O$, 99%), ferrous chloride tetrahydrate ($FeCl_2$•$4H_2O$, 99%), sodium hydroxide (NaOH), trisodium citrate, acrylic acid (AA), potassium persulfate (KPS) and sodium dodecyl sulfate (SDS) were purchased from Shanghai Experiment Reagent Co., China. *N, N′*-methylenebisacrylamide (BIS, 99%), *N*-isopropylacrylamide (NIPAM, 98%) and sodium 2-acrylamido-2-methylpropane sulfonate (AMPS) were purchased from Sigma-Aldrich. All chemicals were used directly. The deionized (DI) water used in the experiments was produced by a water purification system (Pcdx-j-20, Pincheng, China).

Preparation of Fe_3O_4 nanoparticles

Fe_3O_4 nanoparticles were prepared by a simple co-precipitation method described elsewhere.[41,42] Firstly, a certain amount of $FeCl_2$•$4H_2O$ and $FeCl_3$•$6H_2O$ with a molar Fe^{2+}/Fe^{3+} ratio of 1:2 were dissolved into 300 mL DI water under nitrogen atmosphere. Then, 600 μL sodium hydroxide (10 mol/L) were added into the above solution. After stirring for 1 h at room temperature, the reduction system was heated to 90 °C and then 300 mL trisodium citrate (0.3 mol/L) were poured into and stirring for another 1 h under nitrogen atmosphere. Subsequently, the resultant MNPs were collected with the help of a magnet and washed for three times to remove un-reacted compounds. Finally, the obtained MNPs were re-dispersed in water and the dispersion was adjusted to 3.0 wt% for further use.

Preparation of magnetic nanogels

The Fe_3O_4@P(NIPAM-*co*-AMPS) nanogels were synthetized *via* physical encapsulation and precipitation polymerization.[42] In a typical reaction, comonomers NIPAM (1.738 g)and AMPS (2.92 mL), crosslinker BIS (0.148 g), SDS (0.060 g), and Fe_3O_4 magnetic fluid (1 mol% of all the comonomers) were dissolved in 300 mL water in a three-necked round-bottom flask equipped with a reflux condenser. The reaction system were purged with nitrogen to remove oxygen for at least 0.5 h and then heated to 70 °C with mechanical stirring. KPS (0.162 g) was added into the solution to initiate the polymerization reaction. The reaction was continued for 9 h at 70 °C under nitrogen with stirring. Finally, the reaction solution was cooled, and the resultant nanogels were separated from the suspension using a magnet. The obtained precipitate was purified through dialysis against DI water with a dialysis bag (molecular weight cutoff of 12,000 Da) for one week. The dialyzed dispersions and the freeze-dried nanogels were kept for further characterization or use. The Fe_3O_4@P(NIPAM-*co*-AA) nanogels were prepared similarly by replacing AMPS with AA according to the above method and used as a reference.

Characterization of magnetic nanogels

The functional groups of these nanogels were confirmed with Fourier-transform infrared spectroscopy (FTIR, VERTEX 70, BRUKER, Germany) using a solid KBr method.[43] The morphologies of the prepared MNPs and nanogels were observed using a transmission electron microscopy (TEM, H-7000FA, HITACHI, Japan) at the accelerating voltage of 75 kV. Samples were spread onto the surface of a carbon coated copper grid respectively and stained with phosphotungstic acid except Fe_3O_4 nanoparticles. These samples were allowed to dry at room temperature before TEM test. The average hydrated diameters of Fe_3O_4@P(NIPAM-*co*-AMPS) nanogels at different temperatures were determined by dynamic light scattering (DLS, Particle Size Analyzer LB-550, HORIBA Ltd., Japan). Before measurement, the magnetic nanogels were diluted with DI water. The crystal structures of prepared MNPs and magnetic nanogels were studied on an X-ray diffraction (XRD, D8-Focus, BRUKER, Germany) in a 2θ range from 15.0° to 70.0° using a Cu-Kα radiation. A vibrating sample magnetometer (VSM, model 7404, Lake Shore Cryotronics Inc., USA) was used to characterize the magnetic properties of the prepared MNPs and magnetic nanogels. The osmotic pressures of Fe_3O_4@P(NIPAM-*co*-AMPS) nanogels draw solutions were measured by the freezing-point depression method.[43] A precise thermometer was placed in the nanogels dispersion, which was then transferred into a freezer (-20 °C). The temperature profile was recorded to determine the freezing

point temperature T_1 of the dispersion and the value of the solution freezing point depression (ΔT) can be calculated with the freezing point temperature T_0 of pure solvent (DI water). The solution osmotic pressure can be calculated using the equation (1):[43]

$$\pi = \frac{\Delta T}{1.86} \times 17000\ mmHg \qquad \Delta T = T_0 - T_1 \qquad (1)$$

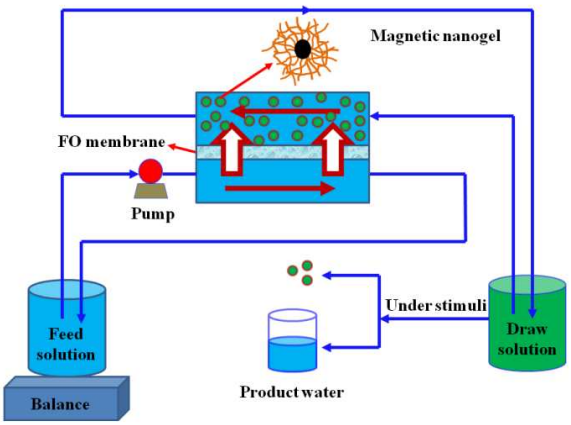

Fig. 1 Schematic diagram of the FO process with magnetic nanogels as draw solute.

FO process

The performances of these magnetic nanogels as draw solute in FO were tested with a lab-scale system (Fig. 1). The permeation cell was designed in a plate and frame configuration with a circular channel (6 cm in diameter, 0.3 cm in height for the feed solution chamber and 10 cm for the draw solution chamber) on both sides of the membrane. The commercially available HTI membrane (Cartridge membrane, Hydration Technologies Inc.) was employed, which was made from cellulose triacetate with an embedded polyester screen mesh. The details of membrane's properties and structure images could be found in the literature.[7,15] The effective membrane area in our experiments was ~23 cm^2. To begin each test, the FO membrane was soaked in DI water for 1 h, and then put in the permeation cell with the shiny side of the membrane facing to the draw solution. DI water (~ 300 mL) was used as a feed solution (FS) and pumped to the cell at a flow rate of 0.064 m/s using a peristaltic pump (WT600-1F, Baoding Longer Precision Pump Co., Ltd). The prepared nanogels dispersions with different concentrations or dry nanogel powders were used as draw solutions, respectively. All the FO processes were carried on at room temperature. The DI water tank was placed on a scale, and the water flux, J_V (unit $Lm^{-2}h^{-1}$, LMH) was calculated according to the equation (2) by measuring the weight change of the FS with time during the test.

$$J_V = \frac{\Delta W}{(A \times \Delta t) \times \rho} \qquad (2)$$

Where, ΔW (g) is the decreasing weight of the FS due to the water permeating through the FO membrane over a predetermined time Δt (min) during FO, A (m^2) is the effective membrane area used in the FO permeate cell and ρ (g/L) is the density of the feed solution and usually assumed as 1000 g/L as the density of water.[18] All these FO tests were carried on in parallel for three times. To recover the nanogels in the draw solution, an external magnet without or with a thermal stimulus at 65 °C was employed to separate the nanogels from water after the above FO process.

Results and Discussion

Preparation and characterization of the magnetic nanogels

To prepare Fe_3O_4@P(NIPAM-*co*-AMPS) nanogels, Fe_3O_4 nanoparticles stabled with trisodium citrate were synthesized firstly by a method of co-precipitation.[41,42] Then, the magnetic nanogels were prepared *via* precipitation polymerization at the present of Fe_3O_4 nanoparticles.[42]

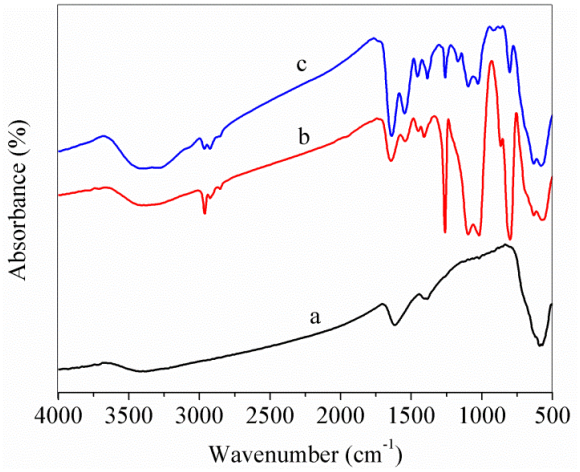

Fig. 2 FTIR spectra of MNPs (a), Fe_3O_4@ P(NIPAM-*co*-AMPS) nanogels (b) and Fe_3O_4@P(NIPAM-*co*-AA) nanogels (c).

The chemical structures of the prepared MNPs, Fe_3O_4@P(NIPAM-*co*-AMPS) nanogels, and Fe_3O_4@P(NIPAM-*co*-AA) nanogels have been confirmed through FTIR spectrum (Fig. 2). In Fig. 2, the peaks located at 572 cm^{-1} can be attributed to the Fe-O group indicating the formation of Fe_3O_4, and the peaks at 1616 cm^{-1} and 1387 cm^{-1} in Fig 2a are caused by the C=O stretching mode, which verify citrate groups attached on the surface of Fe_3O_4 nanoparticles.[41] In Fig. 2b, the peaks at 632 cm^{-1}, 1020 cm^{-1}, and 1261 cm^{-1} are assigned to the S-O stretching, S=O asymmetric stretching, and symmetric stretching of sulfonic acid groups, respectively, indicating the presence of sulfonate group.[44,45] The characteristic peaks appear at 1644 cm^{-1}, 1543 cm^{-1} and 1409 cm^{-1} are ascribed to the secondary amide C=O stretching, secondary amide N-H stretching, and the C-H stretching vibration of $-CH(CH_3)_2$, respectively, which come from NIPAM comonomer. These peaks also appear in the spectrum of Fe_3O_4@P(NIPAM-*co*-AA) nanogels. In the spectrum of Fe_3O_4@P(NIPAM-*co*-AA) nanogels (Fig. 2c), the characteristic peaks at 1170 cm^{-1} and 1639 cm^{-1} correspond to the C-O stretching and C=O stretching of AA units.[46]

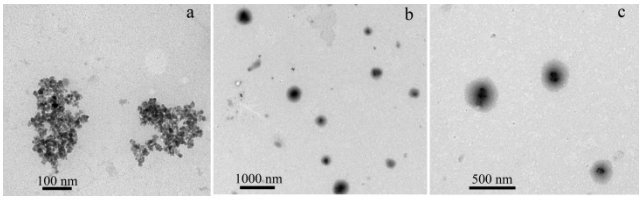

Fig. 3 TEM images of MNPs (a) and P(NIPAM-*co*-AMPS) nanogels (b, c).

The TEM image of Fe_3O_4 nanoparticles is shown in Fig. 3a. It shows the diameter of MNPs is 10-20 nm. Fig. 3b and 3c show the spherical morphology of Fe_3O_4@P(NIPAM-*co*-AMPS) nanogels. They also show that the prepared Fe_3O_4@P(NIPAM-*co*-AMPS) nanogels have a core-shell structure, namely, MNPs as a core (dark center) coated with soft P(NIPAM-*co*-AMPS) shell (grey outer layer). The thick polymer shell on the MNPs may promise to hinder MNPs aggregated, absorb water and generate osmotic pressure in the FO process.

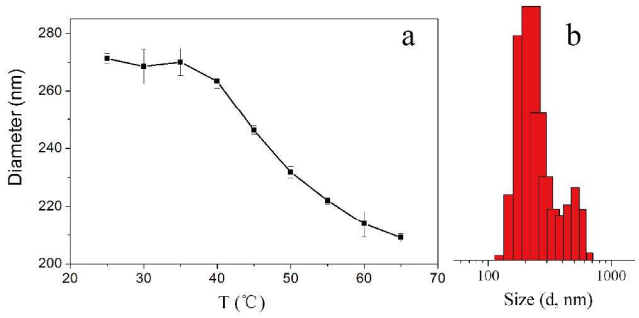

Fig. 4 (a) Average hydrated diameter changed with temperature of Fe_3O_4@P(NIPAM-*co*-AMPS) nanogels and (b) nanogels' size distribution at 25 °C based on intensity.

Fig. 4a shows the effect of temperature on the average hydrated diameter of Fe_3O_4@P(NIPAM-*co*-AMPS) nanogels with the molar ratio of NIPAM and AMPS as 2:1. And Fig. 4b shows the distribution of the nanogels' diameters based on intensity. It can be seen that the average hydrated diameter of the nanogels is 271 nm at 25 °C with narrow distribution (Fig. 4b) and becomes smaller as the temperature increases, which is mainly due to the presence of thermo-responsive PNIPAM segment in the nanogels network.[42] When the temperature is increased, the hydrophobic effect in the Fe_3O_4@P(NIPAM-*co*-AMPS) nanogels will be enhanced, which is induced by the isopropyl groups in the PNIPAM, resulting in the formation of some hydrophobic micro-domain in the nanogles to prompt the water expelled from the nanogels' network.[28,42] That would be benefit to the recovery of these nanogels from the diluted draw solution after FO process under a combined stimuli of heating and magnetic field. It is worth to note that multi-magnetic-separation was used to purify and recover the prepared nanogels from the reactive system. Therefore, the data in Fig. 4 also demonstrate the good redispersibility and thermosensitivity of nanogles in water after several recycles.

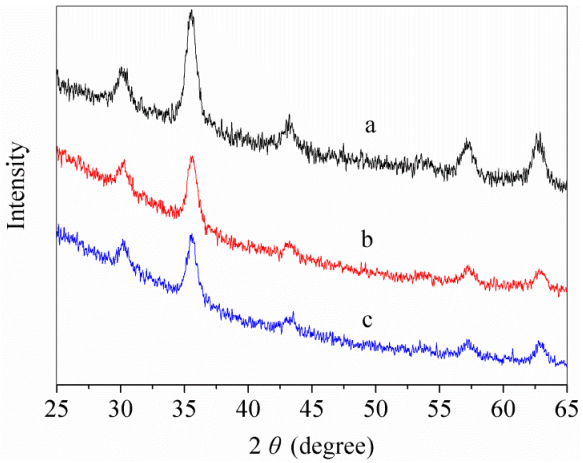

Fig. 5 XRD patterns of MNPs (a), Fe_3O_4@P(NIPAM-*co*-AMPS) nanogels (b) and Fe_3O_4@ P(NIPAM-*co*-AA) nanogels (c).

The X-ray diffraction patterns of MNPs, Fe_3O_4@P(NIPAM-*co*-AMPS) nanogels, and Fe_3O_4@P(NIPAM-co-AA) nanogels are shown in Fig. 5. These results show that the positions and relative intensities of the diffraction peaks in both MNPs and magnetic nanogels are matched well with the standard Fe_3O_4 peaks (JCPDS 01-088-0351).[47] There are mainly six diffraction peaks at 2θ of 30.23°, 35.65°, 43.27°, 53.57°, 57.26° and 62.83°, corresponding to the indices of (220), (331), (400), (422), (511), and (440), respectively.[47] These data reveal that MNPs are Fe_3O_4 with crystal structure, and P(NIPAM-*co*-AMPS) and P(NIPAM-*co*-AA) coated on MNPs do not influence MNPs' crystal structure.

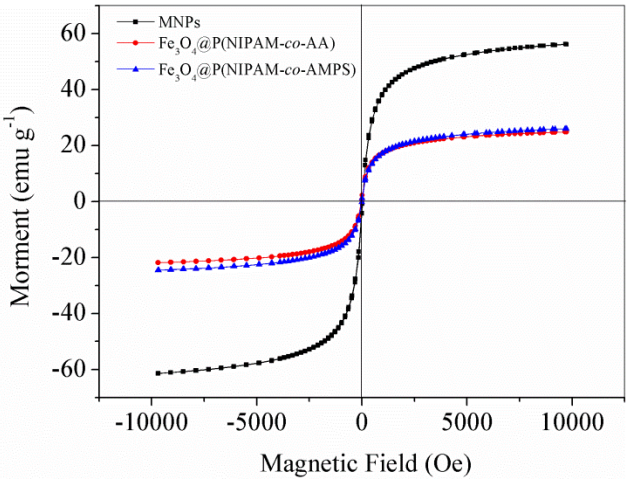

Fig. 6 Magnetization curves of MNPs (black line), Fe_3O_4@P(NIPAM-*co*-AMPS) nanogels (blue line) and Fe_3O_4@ P(NIPAM-*co*-AA) nanogels (red line).

The magnetization curves of Fe_3O_4@P(NIPAM-*co*-AMPS) nanogels and Fe_3O_4@P(NIPAM-*co*-AA) nanogels compared with pure MNPs are shown in Fig. 6. It is seen that the magnetizations of all nanoparticles increase with the strength of the external magnetic field. There is no remanence indicated from the hysteresis loops at a low magnetic field, namely, MNPs and the two kinds of magnetic nanogels possess superparamagnetic property.[48] The saturation magnetization of pure MNPs,

Fe_3O_4@P(NIPAM-*co*-AMPS) nanogels, and Fe_3O_4@P(NIPAM-*co*-AA) nanogels are 58.823, 25.296, and 23.342 emu g^{-1}, respectively. The saturation magnetization of magnetic nanogels is lower than that of pure MNPs, which is attributed to the existence of polymer hydrogels coated on the surface of Fe_3O_4 nanoparticles. However, the saturation magnetization of magnetic nanogels is still high, which will be very beneficial to recover these nanogels under a low magnetic field and reuse them as draw agents in FO. In addition, the superparamagnetic property of the mangentic nanogels will enable them to be redispersed quickly after the removal under an external magnetic field.

The osmotic pressure of poly(NIPAM-*co*-AMPS) nanogels (0.1 g/mL) measured by the method of freezing-point depression is 3.35 bar. The rather low osmotic pressure may due to the nanogels dispersion used in the test with a low concentration in a well-swollen state and the osmotic pressure mainly produced by the dissociation of ionic groups. Much more work should be done to optimize the magnetic nanogels further.

FO performance

The water fluxes of Fe_3O_4@P(NIPAM-*co*-AMPS) nanogels and Fe_3O_4@P(NIPAM-*co*-AA) nanogels used as draw agents are shown in Fig. 7. The results show that the strong ionic Fe_3O_4@P(NIPAM-*co*-AMPS) nanogels dispersion with the concentration of 0.02 g/mL produces an average water flux of 0.26 LMH within the initial 20 min, which is higher than that of weak ionic Fe_3O_4@P(NIPAM-*co*-AA) nanogels (0.11 LMH) with the same nanogels concentration. This may be ascribed to several reasons. First, the strongly ionic sulfonate groups in Fe_3O_4@P(NIPAM-*co*-AMPS) nanogels are completely dissociated, resulting in the generation of higher osmotic pressure than that of weak carboxylate groups with limited dissociation in Fe_3O_4@P(NIPAM-*co*-AA) nanogels. Second, the polymer chains in Fe_3O_4@P(NIPAM-*co*-AMPS) nanogels have the tendency to extend completely due to the strong electrostatic repulsion between strong ionic sulfonate groups,[49] which may leads their bigger equilibrium swelling ratio and more water molecules permeating into the nanogels' network compared with Fe_3O_4@P(NIPAM-*co*-AA) nanogels.

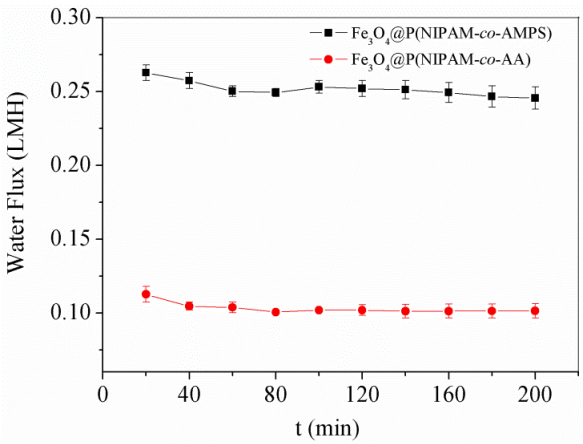

Fig. 7 Water flux of magnetic nanogels as draw solute in FO process at room temperature with the nanogels concentration of 0.02 g mL^{-1}.

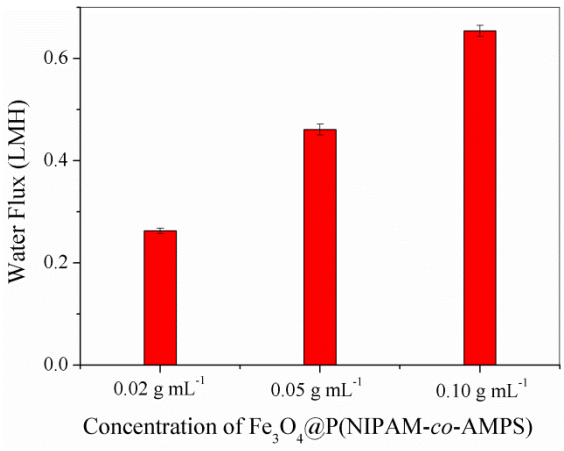

Fig. 8 Effect of Fe_3O_4@P(NIPAM-*co*-AMPS) nanogels concentration in the draw solution on the water flux.

To further investigate the performance of Fe_3O_4@P(NIPAM-*co*-AMPS) nanogels as draw agents in FO, we also study the effect of concentration of Fe_3O_4@P(NIPAM-*co*-AMPS) nanogels in the draw solution on the water flux. As seen in Fig. 8, the average water fluxes are 0.26, 0.46, and 0.65 LMH respectively within the initial 20 min, corresponding to the concentration of the magnetic nanogels of 0.02, 0.05, and 0.10 g mL^{-1}. It is clearly that the water flux increases with an increasing concentration of Fe_3O_4@P(NIPAM-*co*-AMPS) nanogels. This is mainly because that the draw solution with a higher nanogels concentration may produce a higher osmotic pressure.

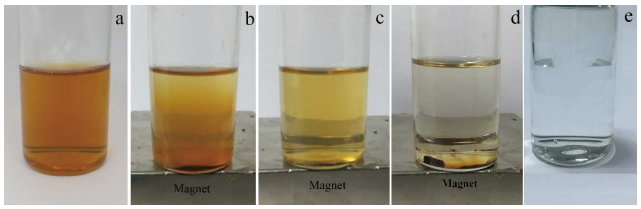

Fig. 9 Photographs of magnetic nanogels dispersion. (a) original state, (b) under an external magnetic stimulus after 20 min at room temperature, (c) under an external magnetic stimulus after 20 min at 65 °C, (d) under an external magnetic stimulus after a week at 65 °C and (e) colorless transparent product obtained after ultrafiltration.

To explore the recyclability of Fe_3O_4@P(NIPAM-*co*-AMPS) nanogels as draw agents in FO, these nanogels were recovered using a magnet made of RuFeB with the magnetic intensity of about 250 mT measured by a Handheld Gassmeter (G100, Coliy Technology GmbH, Germany), or using a combined stimulus of the magnet and heating (65 °C) after FO. As seen in Fig. 9a, the original Fe_3O_4@P(NIPAM-*co*-AMPS) nanogels dispersion is dark yellow. However, when the external magnet is placed, the magnetic nanogels are attracted and move toward to the magnet and the dispersion becomes clearer at last under an external magnetic stimulus after a week at 65 °C (Fig. 9d). Compared with the case in room temperature (Fig. 9b), the magnetic nanogels are easier to be precipitated towards the magnet at 65 °C, and a clearer supernatant can be obtained (Fig. 9c). These results

indicate that the recovery efficiency of the magnetic nanogels under the combined stimuli of heating and magnetic field is higher than that under magnetic field stimulus alone. This may be ascribed to thermosensitive monomer NIPAM introduced into the Fe_3O_4@P(NIPAM-*co*-AMPS) nanogels. As mentioned before, when the temperature is increased, the hydrophobic effect in the Fe_3O_4@P(NIPAM-*co*-AMPS) nanogels woud be enhanced and prompt the water expelled from the nanogels' network. In addition, the hydrophobic interaction between nanogels particles also increases with the increase of temperature, which may makes the nanogels accumulate easily and a quick separation from water. So, the recovery efficiency of Fe_3O_4@P(NIPAM-*co*-AMPS) nanogels as draw agents is improved. It is noted that this thermal stimulus can be come from waste energy in industrial plants or solar power to minimize energy cost. However, for time-saving, it is encouraged to recovery the magnetic P(NIPAM-*co*-AMPS) nanogels from the diluted draw solution by using magnetic stimulus with mild heating and followed by ultrafiltration[22,50] or microfiltration.[51] The colorless transparent product-water has been obtained after ultrafiltration using a Microcon tube (Millipore, 3K MWCO) operating at 8000 rpm for 10 min (Fig. 9e).

Conclusions

In summary, we have prepared the magnetic thermoresponsive ionic Fe_3O_4@P(NIPAM-*co*-AMPS) nanogels *via* physical encapsulation and precipitation polymerization. These magnetic nanogels have a core-shell structure composed with a core of MNPs and a shell of P(NIPAM-*co*-AMPS) and possess thermosensitive and superparamagnetic properties. In addition, Fe_3O_4@P(NIPAM-*co*-AMPS) nanogels can produce a significantly higher water flux than that of Fe_3O_4@P(NIPAM-*co*-AA) nanogels due to the introduced strong ionic monomer AMPS in the former nanogels. And the water flux is enhanced with an increasing concentration of Fe_3O_4@P(NIPAM-*co*-AMPS) nanogels in the draw solution. Furthermore, due to the assistance of thermal stimuli-induced nanogels' shrinkage, the magnetic nanogels could be quickly separated from water under the combined stimuli of heating and magnetic field, resulting in improving the recovery efficiency and reducing energy consumption for reuse. However, there is still much further work to improve the performance of the magnetic nanogels as draw agents in FO, such as how to enhance the osmotic pressure further, and how to use heat from waste energy in industrial plants or solar power to minimize energy cost for recovery and reuse. This work will encourage further development of applying intelligent nanogels as draw agents in FO.

Acknowledgements

We would like to thank the National Natural Science Foundation of China (No. 51308239 and 51103051). We also thank the Analytical and Testing Centre of Huazhong University of Science and Technology for the related measurements.

Notes and references

[a]*School of Environmental Science and Technology, Huazhong University of Science and Technology, Wuhan 430074, China.*
[b]*School of Chemistry and Chemical Engineering, Huazhong University of Science and Technology, Wuhan 430074, China.*
[c]*Department of Civil Engineering, University of Nebraska-Lincoln, Lincoln, NE 68588, USA.*
**Corresponding author: Qin Wang (E-mail: qwang@hust.edu.cn).*

1 M. Elimelech and W. A. Phillip, *Science*, 2011, **333**, 712.
2 T.-S. Chung, S. Zhang, K. Y. Wang, J. Su and M. M. Ling, *Desalination*, 2012, **287**, 78.
3 S. Zhao, L. Zou, C. Y. Tang and D. Mulcahy, *J. Membr. Sci.*, 2012, **396**, 1.
4 Q. Ge, M. Ling and T.-S. Chung, *J. Membr. Sci.*, 2013, **442**, 225.
5 L. Chekli, S. Phuntsho, H. K. Shon, S. Vigneswaran, J. Kandasamy and A. Chanan, *Desalin. Water Treat.*, 2012, **43**, 167.
6 R. L. McGinnis and M. Elimelech, *Desalination*, 2007, **207**, 370.
7 J. R. McCutcheon, R. L. McGinnis and M. Elimelech, *J. Membr. Sci.*, 2006, **278**, 114-123.
8 Z. Liu, H. Bai, J. Lee and D. D. Sun, *Energy Environ. Sci.*, 2011, **4**, 2582.
9 S. Phuntsho, H. K. Shon, S. Hong, S. Lee and S. Vigneswaran, *J. Membr. Sci.*, 2011, **375**, 172.
10 K. S. Bowden, A. Achilli and A. E. Childress, *Bioresour. Technol.*, 2012, **122**, 207.
11 S. K. Yen, F. Mehnas Haja N, M. Su, K. Y. Wang and T.-S. Chung, *J. Membr. Sci.*, 2010, **364**, 242.
12 M. L. Stone, C. Rae, F. F. Stewart and A. D. Wilson, *Desalination*, 2013, **312**, 124.
13 M. L. Stone, A. D. Wilson, M. K. Harrup and F. F. Stewart, *Desalination*, 2013, **312**, 130.
14 Q. Ge and T. S. Chung, *Chem. Commun.*, 2013, **49**, 8471.
15 J. Duan, E. Litwiller, S.-H. Choi and I. Pinnau, *J. Membr. Sci.*, 2014, **453**, 463.
16 N. T. Hau, S.-S. Chen, N. C. Nguyen, K. Z. Huang, H. H. Ngo and W. Guo, *J. Membr. Sci.*, 2014, **455**, 305.
17 K. Lutchmiah, L. Lauber, K. Roest, D. J. H. Harmsen, J. W. Post, L. C. Rietveld, J. B. van Lier and E. R. Cornelissen, *J. Membr. Sci.*, 2014, **460**, 82.
18 H. Bai, Z. Liu and D. D. Sun, *Sep. Purif. Technol.*, 2011, **81**, 392.
19 M. M. Ling, K. Y. Wang and T. S. Chung, *Ind. Eng. Chem. Res.*, 2010, **49**, 5869.
20 M. M. Ling, T. S. Chung and X. Lu, *Chem. Commun.*, 2011, **47**, 10788.
21 Q. Ge, J. Su, T. S. Chung and G. Amy, *Ind. Eng. Chem. Res.*, 2011, **50**, 382.
22 M. M. Ling and T.-S. Chung, *Desalination*, 2011, **278**, 194.
23 M. M. Ling and T.-S. Chung, *Ind. Eng. Chem. Res.*, 2012, **51**, 15463.
24 Q. Zhao, N. Chen, D. Zhao and X. Lu, *ACS Appl. Mater. Interfaces*, 2013, **5**, 11453.
25 R. Ou, Y. Wang, H. Wang and T. Xu, *Desalination*, 2013, 3**18**, 48.
26 Y. Cai, W. Shen, S. L. Loo, W. B. Krantz, R. Wang, A. G. Fane and X. Hu, *Water Res.*, 2013, **47**, 3773.
27 H. Luo, Q. Wang, T. Tao, T. C. Zhang and A. Zhou, *J. Environ. Eng.*, 2014, doi: 10.1061/(ASCE)EE.1943-7870.0000875.
28 D. Li, X. Zhang, J. Yao, G. P. Simon and H. Wang, *Chem. Commun.*, 2011, **47**, 1710.
29 A. Razmjou, Q. Liu, G. P. Simon and H. Wang, *Environ. Sci. Technol.*, 2013, **47**, 13160.
30 D. Li, X. Zhang, J. Yao, Y. Zeng, G. P. Simon and H. Wang, *Soft Matter*, 2011, **7**, 10048.
31 D. Li, X. Zhang, G. P. Simon and H. Wang, *Water Res.*, 2013, **47**, 209.
32 Y. Zeng, L. Qiu, K. Wang, J. Yao, D. Li, G. P. Simon, R. Wang and H. Wang, *RSC Advances*, 2013, **3**, 887.
33 A. Razmjou, G. P. Simon and H. Wang, *Chem. Eng. J.*, 2013, **215-216**, 913.
34 A. Razmjou, M. R. Barati, G. P. Simon, K. Suzuki and H. Wang, *Environ. Sci. Technol.*, 2013, **47**, 6297.
35 D. Li and H. Wang, *J. Mater.Chem. A*, 2013, **1**, 14049.
36 M. A. Ward and T. K. Georgiou, *Polymers*, 2011, **3**, 1215.
37 K. Ogawa;, A. Nakayama; and E. Kokufuta;, *Langmuir*, 2003, **19**, 3178.
38 Q. Wang, H. Xu, X. Yang and Y. Yang, *Int. J. Pharm.*, 2008, **361**, 189.
39 M. Du, D. Lu and Z. Liu, *J. Mol. Catal. B: Enzym.*, 2013, **88**, 60.

40 H. Senff, and W. Richtering, *Colloid Polym. Sci.*, 2000, **278**, 830.
41 D. Yang, J. Hu, and S. Fu, *J. Phys. Chem. C*, 2009, **113**, 7646.
42 T. Fan, M. Li, X. Wu, M. Li and Y. Wu, *Colloids Surf. B: Biointerfaces*, 2011, **88**, 593.
43 J. Duan, E. Litwiller, S. Choi and I. Pinnau, *J. Membr. Sci.* 2014, **453**, 463.
44 S. Durmaz and O. Okay, *Polymer*, 2000, **41**, 3693.
45 A. M. Atta, *J. Appl. Polym. Sci.*, 2012, **124**, 3276.
46 F.-Y. Chou, J.-Y. Lai, C.-M. Shih, M.-C. Tsai, and S. J. Lue, *Colloids Surf. B: Biointerfaces*, 2013, **104**, 66.
47 L. Jiang, Q. Zhou, K. Mu, H. Xie, Y. Zhu, W. Zhu, Y. Zhao, H. Xu and X. Yang, *Biomaterials*, 2013, **34**, 7418.
48 L. Sun, C. Huang, T. Gong and S. Zhou, *Mater. Sci. Eng., C*, 2010, **30**, 583.
49 J. Travas-Sejdic, and A. Easteal, *Polym. Gels Networks*, 1997, **5**, 481.
50 Q. P. Zhao, N. P. Chen, D. L. Zhao and X. M. Lu, *ACS Appl. Mater. Interface*, 2013, **5**, 11453.
51 J. J. Kim, J. S. Chung, H. Kang, Y. A. Yu, W. J. Choi, H. J. Kim and J. C. Lee, *Macromol. Res*., 2014, **22**, 963.